IOP Publishing Journal of Optics A: Pure and Applied Optics
J. Opt. A: Pure Appl. Opt. **9** (2007) S294–S300 doi:10.1088/1464-4258/9/9/S03

Peculiarities of light scattering by nanoparticles and nanowires near plasmon resonance frequencies in weakly dissipating materials

B S Luk'yanchuk[1], M I Tribelsky[2], V Ternovsky[3], Z B Wang[4], M H Hong[1], L P Shi[1] and T C Chong[1]

[1] Data Storage Institute, Agency for Science, Technology and Research, 117608, Singapore
[2] Moscow State Institute of Radioengineering, Electronics and Automation (Technical University), 78 Vernadskiy Avenue, Moscow 119454, Russia
[3] M V Lomonosov Moscow State University, Faculty of Computing Mathematics and Cybernetics, MSU, Vorobjovy Gory, Moscow 119899, Russia
[4] School of Mechanical, Aerospace and Civil Engineering, University of Manchester, Manchester M60 1QD, UK

E-mail: Boris_L@dsi.a-star.edu.sg

Received 3 February 2007, accepted for publication 12 April 2007
Published 22 August 2007
Online at stacks.iop.org/JOptA/9/S294

Abstract
Light scattering by a small spherical particle and nanowire with low dissipation rates are discussed according to the Mie theory (and similar solution for the cylinder). It is shown that near plasmon (polariton) resonance frequencies one can see non-Rayleigh anomalous light scattering with quite a complicated near-field energy flux.

Keywords: plasmon polariton resonance, anomalous light scattering, near-field energy flux

(Some figures in this article are in colour only in the electronic version)

1. Introduction

Light scattering by small particles is an important problem for modern applications in plasmonics and nanotechnologies [1]. However the majority of research on plasmonics was done for materials with rather a strong dissipation at plasmon (polariton) resonance frequencies, e.g. gold, platinum, etc. In this case light scattering by nanostructures can be analysed at the dipole approximation (the Rayleigh scattering), i.e. a point dipole for spheres and a linear dipole for nanowires. At the same time it is well known that all transverse electromagnetic modes for the particle have finite lifetimes because of radiative damping, see [2]. The Rayleigh scattering is valid provided the radiative damping is negligible compared to dissipative losses [3–5]. Meanwhile a few publications devoted to the study of the opposite limit [6–13] clearly show that light scattering in this case is characterized by very unusual properties. In this paper we refer to certain new aspects of light scattering in materials with weak dissipation rates.

2. Optical resonances for volume and surface modes

Though light scattering by a spherical particle is one of the most fundamental problems of classical electrodynamics, the general physical understanding of the problem has not changed much since the publication of its exact solution by Mie in 1908 [14]. As for light scattering by a particle whose size is much smaller than the wavelength of incident light, its understanding up to now is based upon the approach developed by Lord Rayleigh in 1871 [15]. According to the approach a small particle should emit electromagnetic radiation as an oscillating electric dipole. The point to be made is that this simple description has quite a general and very important exception, when the scattering process has

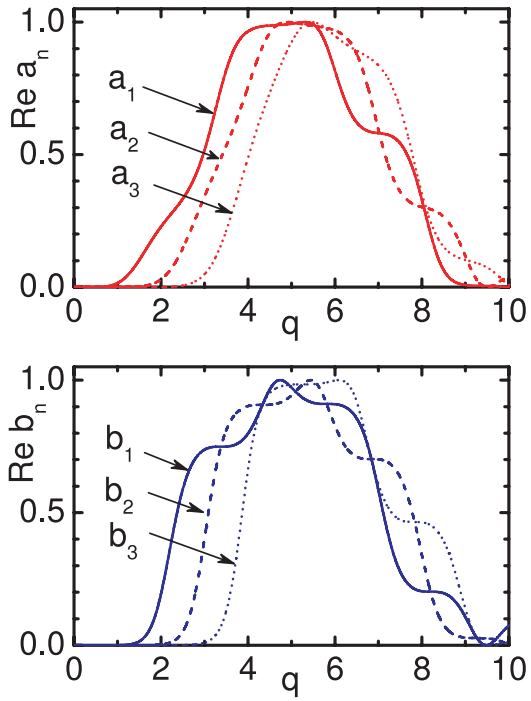

Figure 1. Amplitudes of the first three optical resonances a_ℓ (electric) and b_ℓ (magnetic) for nondissipative material $\varepsilon'' = 0$, at $n = 1.5$. Optical resonances are reached at the points where $\mathrm{Re}\, a_\ell = 1$ or $\mathrm{Re}\, b_\ell = 1$.

very little in common with the Rayleigh scattering, and the extinction (scattering) cross section differs from that given by the Rayleigh approximation in orders of magnitude. This exception corresponds to the low dissipation limit and will be discussed below.

The formula for the Rayleigh approximation can be easily found from the general Mie solution. According to this solution, the extinction, scattering and absorption cross sections are given by the expression $\sigma = \pi a^2 Q$, where related efficiencies Q are presented as follows [3–5]:

$$Q_{\mathrm{ext}} = \frac{2}{q^2}\sum_{\ell=1}^{\infty}(2\ell+1)\,\mathrm{Re}\,(a_\ell + b_\ell),$$
$$Q_{\mathrm{sca}} = \frac{2}{q^2}\sum_{\ell=1}^{\infty}(2\ell+1)\left\{|a_\ell|^2 + |b_\ell|^2\right\}, \qquad (1)$$
$$Q_{\mathrm{abs}} = Q_{\mathrm{ext}} - Q_{\mathrm{sca}}.$$

Here we consider light scattering by a nonmagnetic ($\mu = 1$) spherical particle of radius a immersed in a transparent medium with purely real positive refractive index n_{m}. The quantity $q = n_{\mathrm{m}} a\omega/c$ represents the size parameter ($q \ll 1$ for a small particle); here c is the speed of light in vacuum and ω stands for the incident light frequency. The scattering amplitudes a_ℓ (electric) and b_ℓ (magnetic) are defined by the Mie formulae; it is convenient to write them in the following way:

$$a_\ell = \frac{\Re_\ell^{(a)}}{\Re_\ell^{(a)} + \mathrm{i}\Im_\ell^{(a)}}, \qquad b_\ell = \frac{\Re_\ell^{(b)}}{\Re_\ell^{(b)} + \mathrm{i}\Im_\ell^{(b)}}, \qquad (2)$$

$$\Re_\ell^{(a)} = \tilde{n}\psi_\ell'(q)\,\psi_\ell(\tilde{n}q) - \psi_\ell(q)\,\psi_\ell'(nq),$$
$$\Im_\ell^{(a)} = \tilde{n}\chi_\ell'(q)\,\psi_\ell(\tilde{n}q) - \psi_\ell'(\tilde{n}q)\,\chi_\ell(q), \qquad (3)$$

$$\Re_\ell^{(b)} = \tilde{n}\psi_\ell'(\tilde{n}q)\,\psi_\ell(q) - \psi_\ell(\tilde{n}q)\,\psi_\ell'(q),$$
$$\Im_\ell^{(b)} = \tilde{n}\chi_\ell(q)\,\psi_\ell'(\tilde{n}q) - \psi_\ell(\tilde{n}q)\,\chi_\ell'(q). \qquad (4)$$

Here $\psi_\ell(z) = \sqrt{\pi z/2}\cdot J_{\ell+\frac{1}{2}}(z)$, $\chi_\ell(z) = \sqrt{\pi z/2}\cdot N_{\ell+\frac{1}{2}}(z)$, where $J_\ell(z)$ and $N_\ell(z)$ are the Bessel and the Neumann functions, respectively. The strokes in formulae (3) and (4) indicate differentiation over the entire argument of the corresponding functions, i.e. $\psi_\ell'(z) \equiv \mathrm{d}\psi_\ell(z)/\mathrm{d}z$, etc; $\tilde{n} = \sqrt{\varepsilon} = n + \mathrm{i}\kappa$ is a relative *complex* refractive index, where ε stands for relative dielectric permittivity: $\varepsilon = \varepsilon_{\mathrm{p}}/\varepsilon_{\mathrm{m}}$; indexes 'p' and 'm' indicate the particle and media, respectively. We consider that both real and imaginary parts of the relative refractive index are positive quantities.

The scattering amplitudes a_ℓ and b_ℓ depend on parameter q and the real and imaginary parts of $\varepsilon = \varepsilon' + \mathrm{i}\varepsilon''$. For fixed ε amplitudes a_ℓ and b_ℓ oscillate versus size parameter q. They reach maximal values at some points (the so-called optical resonances [3–5]). For the case of positive $\varepsilon' > 0$ and nondissipative media these resonances were studied in numerous papers, see e.g. [16], due to their important role in radiation pressure, optical levitation, etc. One can see immediately from equation (2) that, for nondissipative media, maximal values of amplitudes are $a_\ell = 1$ and $b_\ell = 1$. They are reached at the points, where $\Im_\ell^{(a)}(q,\varepsilon) = 0$ and $\Im_\ell^{(b)}(q,\varepsilon) = 0$, respectively. These equations present the trajectories of optical resonances on the $\{q,\varepsilon\}$ plane. At $\varepsilon' > 0$ the optical resonances are related to excitation of volume waves in the spherical cavity. It is important that for any reasonable values of $n = \mathrm{Re}\sqrt{\varepsilon}$ these resonances arise at rather large values of the size parameter $q > 1$ and for this case resonances of electric and magnetic amplitudes are overlapped, see in figure 1.

At $\varepsilon < -1$ other branches of optical resonances related to excitation of surface electromagnetic waves arise. At $q \to 0$ these resonances occur at $\varepsilon = \varepsilon_\ell = -(\ell+1)/\ell$. The branches of volume and surface Mie resonances converge at some negative values of ε, e.g. at $\varepsilon \approx -5$ and $q \approx 1.2$ for dipole resonance $\ell = 1$, see in figure 2.

Expanding the Bessel and Neumann functions in power series, it is easy to find that at small q

$$\Re_\ell^{(a)} \approx q^{2\ell+1}\frac{(\ell+1)}{[(2\ell+1)!!]^2}\tilde{n}^\ell\left(\tilde{n}^2-1\right),$$
$$\Im_\ell^{(a)} \approx \tilde{n}^\ell\frac{\ell}{2\ell+1}\left[\tilde{n}^2 + \frac{\ell+1}{\ell} - \frac{q^2}{2}\left(\tilde{n}^2-1\right)\right.$$
$$\left.\times\left(\frac{\tilde{n}^2}{2\ell+3} + \frac{\ell+1}{\ell\,(2\ell-1)}\right)\right], \qquad (5)$$
$$\Re_\ell^{(b)} \approx -\frac{\tilde{n}q^2}{2\ell+1}\Re_\ell^{(a)},$$
$$\Im_\ell^{(b)} \approx -\tilde{n}^{\ell+1}\left[1 + \frac{1-\tilde{n}^2}{2\,(2\ell+1)}q^2\right].$$

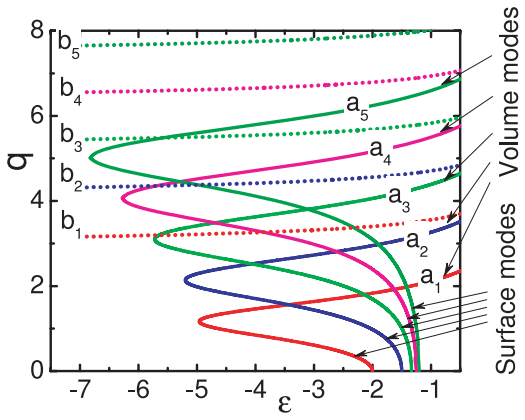

Figure 2. Trajectories of the five first optical resonances a_ℓ (solid) and b_ℓ (dashed) for nondissipative material $\varepsilon'' = 0$, at negative ε.

Far from the resonances $\Re \ll \Im$. In this case the term with $\ell = 1$ (dipole scattering) plays the dominant role. Also for small particles one can neglect magnetic amplitudes compared to the electric ones because of their additional smallness in q. It yields the classical Rayleigh formula:

$$Q_{\text{sca}} \approx \frac{8}{3}\left|\frac{\varepsilon - 1}{\varepsilon + 2}\right|^2 q^4. \tag{6}$$

The Rayleigh scattering approximation for a small particle is applicable for all cases *far from the optical resonances*. Close to the resonances it should be modified, provided the dissipation is small enough (the right-hand side of equation (6) just diverges at $\varepsilon = -2$). Note, there are two possibilities to achieve an optical resonance for small particles. The first way is related to large values of ε. For example, at $\varepsilon = 400$ optical dipole magnetic resonance occurs at $q \approx 0.157$ and dipole electric resonance at $q \approx 0.385$. The other way is to work with negative ε in the vicinity of plasmon (polariton) resonances, where $\varepsilon \approx -(\ell + 1)/\ell$. In this case optical resonances are associated with electric amplitudes solely and correspond to resonant excitation of surface plasmon (polariton) modes.

Pronounced peculiarities of light scattering by small weakly dissipative particles near the plasmon resonance frequencies differ from the Rayleigh case so dramatically that it allows us to name such a scattering 'anomalous scattering' [10, 11, 13]. In anomalous scattering far field one can see the so-called 'inverse hierarchy of optical resonances' [6, 10, 13]. Namely, at the resonance frequencies $\omega = \omega_\ell$ the corresponding electric amplitude $a_\ell = 1$ while b_ℓ is negligibly small. Then, as it follows from equation (1) $Q^{(\ell)}_{\text{sca}} = 2(2\ell + 1)/q^2$, where $Q^{(\ell)}_{\text{sca}}$ stands for the resonance partial efficiency. As in the vicinity of the resonances the net efficiency is overwhelmingly determined by the corresponding partial one the expression $Q^{(\ell)}_{\text{sca}} = 2(2\ell + 1)/q^2$ means the resonance scattering cross section increases with an increase in order of the resonance ℓ. Thus, the cross section at the quadrupole resonance is 5/3 of that at the dipole resonance, etc. However to observe this 'inverse hierarchy' at least the necessary condition $\varepsilon'' \ll 1$ should be satisfied. Usually experiments are carried out with small particles of gold, silver, mercury and platinum [17]. For all these metals the condition of weak dissipation at the resonance frequencies, $\varepsilon''(\omega_\ell) \ll 1$, does not hold. A possible candidate for manifestation of the anomalous scattering may be an additively coloured crystal of KCl with colloidal potassium particles as scatterers [6]. Another possible example discussed in [10] is an aluminium particle in vacuum. The third example is Na (also as colloidal particles in crystals of NaCl with stoichiometric excess of sodium). According to [17] the three materials have weak dissipation rates (about $\varepsilon'' \approx 0.1$) at the frequencies of surface plasmon excitation, i.e. at $\lambda \approx 125$–140 nm for Al, $\lambda \approx 310$–380 nm for Na and $\lambda \approx 500$–550 nm for K. Our calculations with experimental values for the dielectric function show that for Al particles with $a = 30$ nm the ratio of the extinction cross-sections at quadrupole and dipole resonances is about 1.19 [10]. Naturally, it is smaller than 5/3 for a nondissipative particle, but much greater than that for the Rayleigh approximation. In our calculations [10] we took into account the size effect with the help of renormalization of collision frequency of free electrons due to their collisions with the particle surface [18], $\gamma \to \gamma_\infty + v_{\text{F}}/a$. The data for Fermi velocity v_{F} for this renormalization was also taken from the experiment [19].

Optical plasmon resonances for weakly dissipative materials are extremely sharp. In the case of the Rayleigh scattering the width of the resonance line is directly related to ε'' and vanishes at $\varepsilon'' \to 0$. In contrast to that the exact Mie solution at $\varepsilon'' = 0$ near plasmon resonance frequencies yields the usual Lorentzian contour with a certain characteristic width γ_ℓ. To show this let us consider the case of a metallic particle whose dielectric permittivity is described by the Drude formula:

$$\varepsilon = \tilde{n}^2 = 1 - \frac{\omega_{\text{p}}^2}{\omega^2 + \gamma^2} + \text{i}\frac{\gamma}{\omega}\frac{\omega_{\text{p}}^2}{\omega^2 + \gamma^2}. \tag{7}$$

Here, as usual, ω_{p} denotes the plasma frequency, while γ is the frequency of electron collisions. Inserting equation (7) in equation (6) in the Raleigh case one obtains a Lorentzian scattering contour,

$$Q^{(\text{Ra})}_{\text{sca}} = \frac{8}{3}\frac{\omega_{\text{sp}}^4}{\left(\omega^2 - \omega_{\text{sp}}^2\right)^2 + \omega^2\gamma^2} q^4, \tag{8}$$

where $\omega_{\text{sp}} = \omega_{\text{p}}/\sqrt{3}$ stands for frequency of the dipole surface plasmon resonance at $q \to 0$. As is seen from equation (8), the resonance width is directly connected with the parameter responsible for dissipation. The Drude formula can be written in a similar way in the absence of dissipation ($\gamma = 0$). The expression for the partial dipole scattering efficiency following from equation (1) is $Q_{\text{sca}} \approx 6|a_1|^2/q^2$. Here $a_1 = \Re_1^{(a)}/(\Re_1^{(a)} + \text{i}\Im_1^{(a)})$, where $\Re_1^{(a)}$ and $\Im_1^{(a)}$ at $q \ll 1$ are determined from equation (5). We should remember that the plasmon resonance frequencies are defined by the condition $\Im_1^{(a)} = 0$, and therefore, in the nearest vicinity of ω_{sp}, $\Im_1^{(a)} \approx \text{i}\sqrt{2}(\omega^2 - \omega_{\text{sp}}^2)/\omega_{\text{sp}}^2$ and $\Re_1^{(a)} \approx -2\text{i}\sqrt{2}q^3/3$. It yields the following Lorentzian profile:

$$Q_{\text{sca}} = \frac{8}{3}\frac{\omega_{\text{sp}}^4}{\left(\omega^2 - \omega_{\text{sp}}^2\right)^2 + \frac{4}{9}q^6\omega_{\text{sp}}^4} q^4. \tag{9}$$

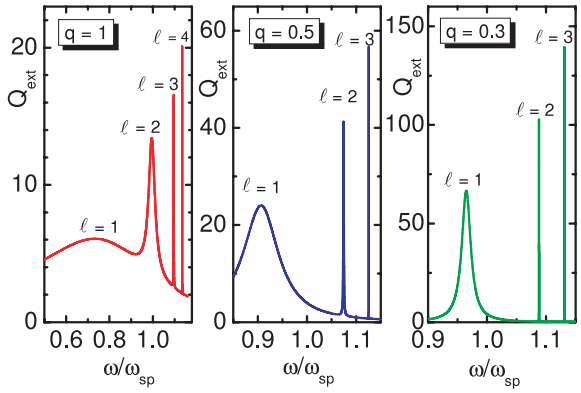

Figure 3. The nondissipative limit for a spherical particle with radius a. Frequency dependence of Q_{ext} for three values of q. Note different scales of vertical axis on different panels. Calculations according to the exact Mie solution; $\varepsilon = 1 - \omega_{\text{p}}^2/\omega^2$, where $\omega_{\text{sp}} = \omega_{\text{p}}/\sqrt{3}$ stands for the frequency of the dipole surface plasmon resonance at $q \to 0$ (ω_{p} is the plasma frequency).

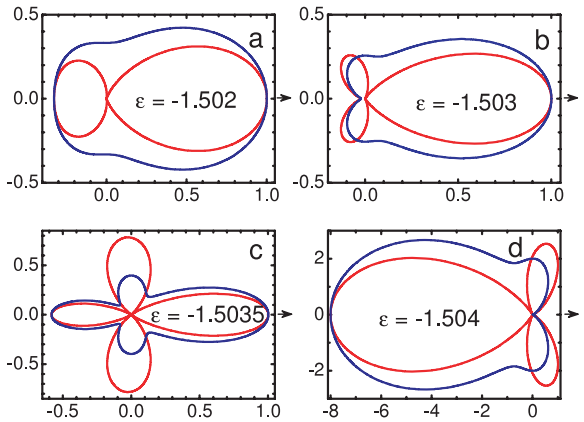

Figure 4. Polar scattering diagrams for the scattering of linearly polarized (red) and nonpolarized (blue) light in the vicinity of quadrupole resonance for the nondissipative small particle with $q = 0.1$ and different values of the dielectric permittivity (shown in the pictures).

Comparing equations (8) and (9), it is easy to see that the role of the dissipation parameter in equation (9) is played by the quantity

$$\gamma_{\text{eff}} = \frac{2}{3}\omega_{\text{sp}} q^3 = \frac{2}{3}\frac{\omega_{\text{sp}}^4 a^3}{c^3}. \tag{10}$$

This damping is related to the finite plasmon lifetime $\tau_{\text{p}} = \gamma_{\text{eff}}^{-1}$ caused by the radiative losses. The effects of a finite plasmon lifetime have already been discussed in the literature. It has been attributed to dissipative (*non-radiative*) losses and for a small particle estimated as $\tau_{\text{p}} \approx a/v_{\text{F}}$, see [18]. In contrast, in our case, the finiteness of the lifetime is attributed to *radiative* (nondissipative) losses due to the transformations of the localized plasmons into scattering light [2, 6, 13] and corresponding time sharply increases with a decrease in the particle size: $\tau_{\text{p}} \propto a^{-3}$. Formula (10) represents the 'natural width' of the dipole resonance related to this transformation. In the general case the natural width of the arbitrary resonance is given by the following expression [13]:

$$\gamma_\ell = \frac{(\ell+1)q^{2\ell+1}}{[\ell(2\ell-1)!!]^2(\mathrm{d}\varepsilon/\mathrm{d}\omega)_\ell}, \tag{11}$$

where derivative $(\mathrm{d}\varepsilon/\mathrm{d}\omega)_\ell$ is taken at the corresponding plasmon resonance frequency $\omega = \omega_\ell$. Note an extremely sharp decrease in γ_ℓ with both a decrease in q and an increase in ℓ, see in figure 3.

However this fascinating effect is strongly suppressed by dissipation. The necessary conditions for the anomalous scattering to come into being may be found from the Mie theory, taking into account the dissipation factor ε'' in the denominator of the scattering amplitude. This consideration leads to the applicability condition [6, 13]

$$\varepsilon''(\omega_\ell) \ll \frac{q^{2\ell+1}}{\ell\,[(2\ell-1)!!]^2}. \tag{12}$$

When this condition is fulfilled the anomalous scattering is dominant. In the opposite case the Rayleigh scattering is restored. This condition clearly explained numerical results found in [10]. For example, it follows from equation (12) that with any small ε'' the anomalous scattering is suppressed for very small particles. Thus, under real experimental conditions anomalous scattering can be realized just in some intermediate range of size parameters and only up to a certain order of the resonances: $\ell < \ell_{\max}$.

Another peculiarity of weakly dissipative material is the extra high sensitivity of the angular distribution of scattering light near plasmon resonance frequency, see figure 4. One can compare this picture with figure 10.14 in [3], where calculations are done for a small gold particle. From figure 4 follows that very small variation in the incident light frequency changes the scattering diagram from forward scattering to backward scattering. Note that for a small perfectly reflected sphere the ratio of forward and backward scattered intensities is 1:9, see problem 2 to § 92 in [20].

For the Rayleigh scattering all components of the scattered fields vanish at $q \to 0$. In contrast, the Mie theory for nondissipative materials near plasmon resonance frequencies yields singularities and divergent fields, proportional to $q^{-\ell-2}$ for $E_{r,\theta,\varphi}^{(\ell)}$ components of the electric field and proportional to $q^{-\ell-1}$ for $H_{\theta,\varphi}^{(\ell)}$ components. This divergence is stabilized at $\varepsilon'' \neq 0$, however the inverse size dependence may result in very large enhancement rates of the fields achieved at a small q.

3. Near-field structure of the energy flux

Though the discussed far-field effects are already quite unusual, the most appealing manifestation of the anomalous scattering takes place in the near field. The key point is that the dramatic changes in both the modulus and phase of complex amplitude a_ℓ in the vicinity of plasmon resonances yield the corresponding dramatic changes in the near-field structure. For the dipole mode at the dipole resonance point ($a_1 = 1$) the exact Mie solution yields the following equation for the field lines at x–z plane: $\mathrm{d}\rho/\mathrm{d}\theta = \rho S_r/S_\theta$, where $\rho = r/a$, and S_r and S_θ are corresponding spherical components of the

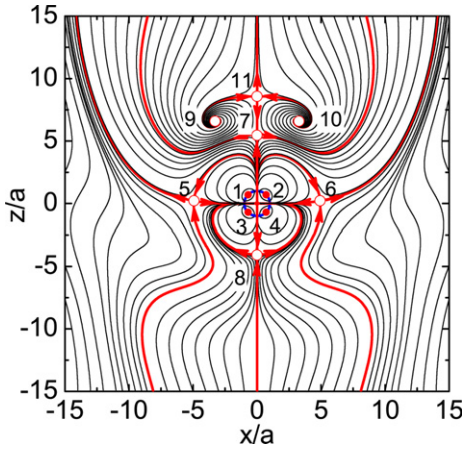

Figure 5. The Poynting vector field in the vicinity of quadrupole resonance at $q = 0.3$ and $\varepsilon = -1.553\ldots$. Various singular points (red circles) are marked with Arabic numerals. The red lines represent the separatrixes; the blue line denotes the particle surface. Points 1–4 indicate the centres of four localized plasmons (polaritons) on the surface of the particle. Within the particle with weak dissipation these points correspond to centres of the 'optical whirlpools' discussed in [9]. Points 5–8 and 11 are saddles. Note two optical vortices (points 9 and 10).

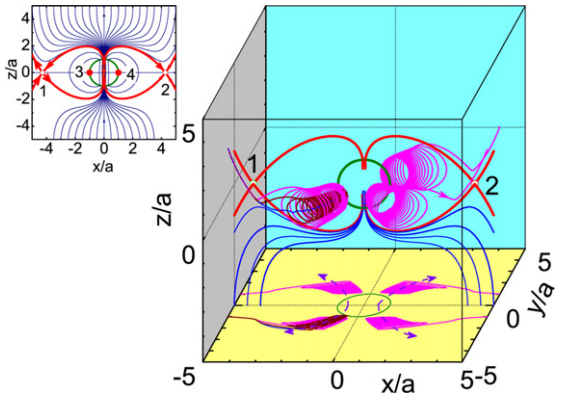

Figure 6. The Poynting vector lines in the vicinity of a spherical particle for the nondissipative case (incident plane wave with electric field polarized along the x axis comes from $z = -\infty$). Left insert shows 2D field in the xz plane. Points 1 and 2 are saddles. Thick red lines indicate separatrixes in the xz plane. Field lines in 2D picture demonstrate circular energy flux around centres (points 3 and 4). In the 3D plot one can see the energy flow outward the particle (helicoidally shaped field lines). It illustrates the radiative losses of energy, general directions of which are shown by arrows on the bottom xy projection plane.

Poynting vector:

$$S_r = \frac{\cos\theta}{2q^3\rho^3}(2q^3\rho^3 - 3q^2\rho^2\cos K + (3 - 3q^2\rho^2)\sin K),$$

$$K = q\rho(1 - \cos\theta),$$

$$S_\theta = \frac{\sin\theta}{2q^4\rho^4}(-2q^4\rho^4 - 9(1 - q\rho)\cos\theta \qquad (13)$$

$$- \ 3q^2\rho^2(2 - q\rho\cos\theta)\cos K$$

$$+ \ 3q\rho(2 + q^2\rho^2\cos\theta)\sin K).$$

At the same time an analogous equation for the field lines at the Rayleigh scattering [21] contains singularities at $\varepsilon'' \to 0$. We should add also that even small deviations of ω from the exact resonance values make the single-partial-mode approximation insufficient to describe the near-field distribution [7].

While the far-field effects are restricted by strong inequality (12) the near-field distribution is affected by the anomalous scattering up to much larger dissipation rates. For example, for a particle with $q = 0.3$ complete restoration of the Rayleigh scattering happens only at $\varepsilon'' > 0.6$ [7]. Modifications of the Poynting vector field and a bifurcation diagram in the vicinity of the dipole resonance have already been discussed in [7, 11, 12]. Here we present a particular example of the Poynting vector field in the vicinity of the quadrupole resonance at $\varepsilon'' = 0$, see figure 5. The Poynting vector field is shown in the xz plane for incident electric field polarized along the x axis, and a wave propagating along the z axis. All the singular points are lying in the near field, i.e. all these field peculiarities have the characteristic scale much smaller than the wavelength. It provides a unique opportunity to control optically field distribution in the nanoscale region.

The radiation losses related to transformation of the plasmon into the propagating electromagnetic radiation can be clearly seen in a 3D picture of the near-field distribution of the Poynting vector in figure 6.

4. Anomalous light scattering by nanowires

Effects related to the radiative damping are important also for nanowires with surface plasmon (polaritons). This also leads to deviation of extinction and scattering characteristics from the Rayleigh approximations for a linear dipole, e.g. for the scattering efficiency [4]

$$\tilde{Q}_{\rm sca}^{(Ra)} = \frac{\pi^2}{4}\left(\frac{\varepsilon - 1}{\varepsilon + 1}\right)^2 q^3. \qquad (14)$$

We used a tilde to distinguish cylindrical geometry. Equation (14) is written in normalized dimensionless units; to find the dimensional cross sections $\sigma_{\rm sca}$, one should multiply $\tilde{Q}_{\rm sca}$ by the geometrical cross section $\sigma_{\rm geom}$. For a cylinder $\sigma_{\rm geom} = 2aL$, where a is the radius of the wire and $L \gg a$ is the length of the cylinder. Quantities q, ε and $\tilde{n}$ have the same meaning as before.

Scattering of light by an infinite cylinder also has the exact solution, similar to the Mie solution for a sphere, see e.g. [4]. The simplest form this solution has is for the normal incidence of radiation and TE-mode. In this case the scattering efficiency is expressed in terms of coefficient $\tilde{a}_\ell$ only [4]:

$$\tilde{Q}_{\rm sca} = \frac{2}{q}\sum_{n=-\infty}^{\infty}|\tilde{a}_n|^2, \qquad \text{where } \tilde{a}_\ell = \frac{\tilde{\Re}_\ell}{\tilde{\Re}_\ell + {\rm i}\tilde{\Im}_\ell}$$

and

$$\tilde{\Re}_\ell = \tilde{n}J_\ell(\tilde{n}q)\,J'_\ell(q) - J'_\ell(\tilde{n}q)\,J_\ell(q), \qquad (15)$$

$$\tilde{\Im}_\ell = \tilde{n}J_\ell(\tilde{n}q)\,N'_\ell(q) - J'_\ell(\tilde{n}q)\,N_\ell(q). \qquad (16)$$

Here $J_\ell(\rho)$ and $N_\ell(q)$ are the Bessel and Neumann functions. Coefficients $\tilde{a}_\ell$ are symmetric: $\tilde{a}_{-\ell} = \tilde{a}_\ell$, In contrast to a spherical particle, where the Mie expansion begins with the dipole term ($\ell = 1$), the cylinder contains the monopole term ($\ell = 0$) also.

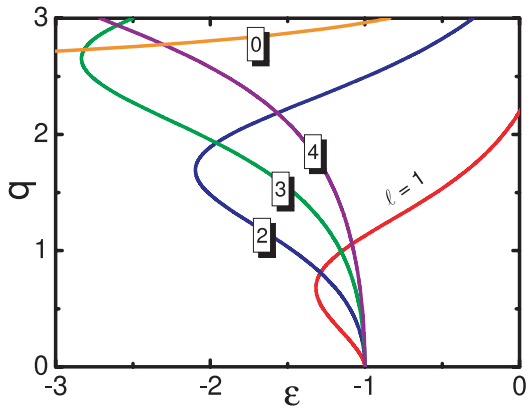

Figure 7. Trajectories of the first resonances ($\ell = 0, 1, 2, 3, 4$) found from the equation $\tilde{\Im}_\ell(\varepsilon, q) = 0$. For the dipole resonance ($\ell = 1$) the surface plasmon branch merges with the volume optical one (for which $\mathrm{d}q(\varepsilon)/\mathrm{d}\varepsilon > 0$) at $q \approx 0.7$ and $\varepsilon \approx -1.3$. The trajectories of all other resonances with $\ell > 1$ demonstrate similar behaviour.

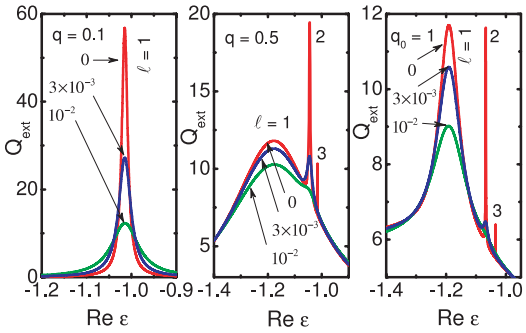

Figure 8. Spectral dependences of extinction efficiencies for an infinite cylinder (TE-mode) with different values of the size parameter: $q = 0.1$ (a), 0.5 (b) and 1 (c). Three curves in each plot correspond to different values of dissipation parameter $\gamma/\omega_\mathrm{p} = 0$, 3×10^{-3} and 10^{-2} in the Drude formula equation (7). For nondissipative material $\gamma = 0$ and $q = 0.5$ and 1.0 the three sequential resonances are seen clearly.

Employing the well-known expansion for the Bessel functions, [22]:

$$J_\ell(z) = \left(\frac{z}{2}\right)^\ell \sum_{p=0}^{\infty} \frac{\left(-\frac{z^2}{4}\right)^p}{p!\Gamma(\ell + p + 1)}, \tag{17}$$

we can obtain the following term in the numerator of $\tilde{a}_\ell$ for the case of small size parameter $q \ll 1$ [12]

$$\tilde{\Re}_\ell \approx \begin{cases} \dfrac{\tilde{n}\left(\tilde{n}^2 - 1\right)}{16} q^3, & \text{if } \ell = 0 \\ \dfrac{\tilde{n}^{\ell-1}\left(\tilde{n}^2 - 1\right)}{2^{2\ell}\ell!\,(\ell-1)!} q^{2\ell-1}, & \text{if } \ell > 0. \end{cases} \tag{18}$$

The corresponding expansion of $\tilde{\Im}_\ell$ in powers of small q contains a product of convergent Bessel functions $J_\ell(q)$ to divergent Neumann functions $N_\ell(q)$. As a result the leading term in this expansion is as follows:

$$\tilde{\Im}_\ell \approx \begin{cases} \dfrac{2\tilde{n}}{\pi q} + \ldots, & \text{if } \ell = 0 \\ \dfrac{\tilde{n}^{\ell-1}\left(\tilde{n}^2 + 1\right)}{\pi q} + \ldots, & \text{if } \ell > 0, \end{cases} \tag{19}$$

where ellipses indicate dropped higher order in q terms. The resonances at $q \to 0$ correspond to $\varepsilon = -1$ for all modes with $\ell \geqslant 1$ in contrast to a spherical particle where all the modes correspond to different resonant frequencies: $\varepsilon = -(\ell + 1)/\ell$. Such degeneracy is removed at finite q when every mode has its individual resonance conditions, see below.

Far from the resonance frequencies the inequality $|\tilde{\Im}_\ell| \gg |\tilde{\Re}_\ell|$ holds, thus, $\tilde{a}_\ell \approx -\mathrm{i}\tilde{\Re}_\ell/\tilde{\Im}_\ell$, which yields

$$\tilde{a}_0 \approx -\mathrm{i}\frac{\pi}{32}(\varepsilon - 1)q^4, \qquad \tilde{a}_\ell \approx -\mathrm{i}\frac{\pi}{2^{2\ell}\ell!(\ell-1)!}\frac{\varepsilon - 1}{\varepsilon + 1} q^{2\ell}, \quad \text{for } \ell > 0. \tag{20}$$

One can see that the dominant term at small q is represented by the dipole partial mode with $\ell = 1$, thus $\tilde{Q}_\mathrm{sca} \approx 4|\tilde{a}_1|^2/q$ and we arrive at the Rayleigh formula equation (14).

However the exact resonances correspond to the situation when $\tilde{\Im}_\ell(\varepsilon, q) = 0$. Thus, accurate description of the resonances requires accounting for the $\tilde{\Re}_\ell$ contribution in the resonant denominators. It results in finite and real values $a_\ell = 1$ at the resonant frequencies even in the absence of the usual dissipation, i.e. at $\mathrm{Im}\,\varepsilon = 0$. For this 'nondissipative' case with $-1 < \varepsilon < 0$ all the amplitudes tend to zero at $q \to 0$. With a larger size parameter these amplitudes demonstrate resonances similar to the Mie resonances for a sphere. For small q resonances arise at $\varepsilon < -1$. They occur just for modes with $\ell \geqslant 1$ and do not happen for the monopole mode $\ell = 0$, see equation (19). These resonances are extremely sharp. The trajectories of the resonances are determined by equation $\tilde{\Im}_\ell(\varepsilon, q) = 0$. To find this equation at small q it suffices to take into account the term proportional to q^2 only. As a result we arrive at the equations

$$\varepsilon + 1 \approx \frac{q^2}{8}(\varepsilon - 1)\left[2 + \varepsilon - 4\log\frac{qC}{2}\right], \qquad \text{for } \ell = 1,$$
$$\varepsilon + 1 \approx \frac{q^2}{4}(\varepsilon - 1)\left[\frac{1}{\ell - 1} + \frac{\varepsilon}{\ell + 1}\right], \qquad \text{for } \ell > 1, \tag{21}$$

where $\log C \equiv \gamma \cong 0.577$ is Euler's constant.

The trajectories of several sequential resonances on the plane of parameters $\{q, \varepsilon\}$ are shown in figure 7. At small q these trajectories are described by equation (21) and tend to limit $\varepsilon = -1$ at $q \to 0$. The amplitudes $\tilde{a}_\ell$ are equal one everywhere along the corresponding trajectories. Resonances at small $q \ll 1$ correspond to localized surface plasmon (polariton) modes. At certain values of ε they converge with volume resonances similar to that for the discussed optical resonances for a sphere, cf figure 2. At small $q \ll 1$ surface plasmon resonances produce an anomalous light scattering effect, see in figure 8.

In the case of the nanowire the near-field structure of the energy flux turns out to be quite sensitive to fine detuning of frequency of the incident light from the exact resonant frequencies. Numerous modifications of the Poynting vector field were discussed in detail in [12].

5. Conclusions

Various applications of the anomalous scattering in nanotechnologies and related fields may be associated with (i) enormous amplification of the incident electromagnetic field in the near field; (ii) controllable changes of the near-field structure with changes of the incident light frequency; (iii) comparable intensity of the resonant electromagnetic field at different resonant frequencies of the incident light, corresponding to different orders of resonance, accompanied by quite a different field distribution for each order of the resonance. All this opens new prospects for optical manipulation in the field structure in the nanoscale region.

Acknowledgments

We are very grateful to S I Anisimov, L P Pitaevskiy and N Arnold for discussions and critical comments. This work was partially supported by Russian Basic Research Foundation (grants 04-02-17225 and 04-02-16972).

References

[1] Barnes W L, Dereux A and Ebbesen T W 2003 Surface plasmon subwavelength optics *Nature* **424** 824–9
[2] Fuchs R and Kliewer K L 1968 Optical modes of vibration in an ionic crystal sphere *J. Opt. Soc. Am.* **58** 319–30
[3] Born M and Wolf E 1999 *Principles of Optics* 7th edn (Cambridge: Cambridge University Press)
[4] Bohren C F and Huffman D R 1998 *Absorption and Scattering of Light by Small Particles* (New York: Wiley)
[5] Hulst van de H C 1981 *Light Scattering by Small Particles* (New York: Dover)
[6] Tribelsky M I 1984 Resonant scattering of light by small particles *Sov. Phys.—JETP* **59** 534–6
[7] Wang Z B, Luk'yanchuk B S, Hong M H, Lin Y and Chong T C 2004 Energy flows around a small particle investigated by classical Mie theory *Phys. Rev.* B **70** 035418
[8] Evlyukhin A B and Bozhevolnyi S I 2005 Applicability conditions for the dipole approximation in the problems of scattering of surface plasmon polaritons *JETP Lett.* **81** 218–21
[9] Bashevoy M V, Fedotov V A and Zheludev N I 2005 Optical whirlpool on an absorbing metallic nanoparticle *Opt. Express* **13** 8372–9
[10] Luk'yanchuk B S and Tribelsky M I 2005 Anomalous light scattering by small particles and inverse hierarchy of optical resonance *Collection of Papers Devoted to Memory of Prof. M N Libenson St.-Petersburg Union of the Scientists Russia 101–15*
[11] Luk'yanchuk B S, Tribelsky M I and Ternovsky V 2006 Light scattering at nanoparticles close to plasmon resonance frequencies *J. Opt. Technol.* **73** 371–7
[12] Luk'yanchuk B S and Ternovsky V 2006 Light scattering by thin wire with surface plasmon resonance: bifurcations of the Poynting vector field *Phys. Rev.* B **73** 235432
[13] Tribelsky M I and Luk'yanchuk B S 2006 Anomalous light scattering by small particles *Phys. Rev. Lett.* **97** 263902
[14] Mie G 1908 Beiträge zur Optik trüber Medien, speziell kolloidaler Metallösungen *Ann. Phys.* **25** 377–445
[15] Lord Rayleigh 1871 On the light from the sky, its polarization and colour appendix *Phil. Mag.* **41** 107–20
Lord Rayleigh 1871 On the light from the sky, its polarization and colour appendix *Phil. Mag.* **41** 274–9
Lord Rayleigh 1871 On the scattering of light by small particles *Phil. Mag.* **41** 447–54
[16] Kerker M 1989 Selected papers on light scattering *Proc. SPIE* **951** 283–330
[17] Palik E D 1985 *Handbook of Optical Constants of Solids* (New York: Academic)
[18] Kreibig U and Vollmer M 1995 *Optical Properties of Metal Clusters* (Berlin: Springer)
[19] Wegehaupt T and Doezema R E 1977 Measurement of the anisotropic Fermi velocity in Al *Phys. Rev.* B **16** 2515–25
[20] Landau L D and Lifshitz E M 2002 *Electrodynamics of Continuous Media* (Oxford: Butterworth-Heinemann)
[21] Bohren C F 1983 How can a particle absorb more than the light incident in? *Am. J. Phys.* **51** 323–7
[22] Jahnke E, Emde F and Lösch F 1960 *Tables of Higher Functions* 6th edn (New York: McGraw-Hill)